Three-Dimensional Breathhold Magnetization-Prepared TrueFISP:

A Pilot Study for Magnetic Resonance Imaging of the Coronary Artery Disease

Richard M. McCarthy, MD[*], **Vibhas S. Deshpande, PhD**[*,†], **Nirat Beohar, MD**[‡], **Sheridan N. Meyers, MD**[‡], **Steven M. Shea, PhD**[*,†], **Jordin D. Green, PhD**[*,†], **Xin Liu, MD**[*], **Xiaoming Bi, PhD**[*,†], **F. Scott Pereles, MD**[*], **John Paul Finn, MD**[*], **Charles J. Davidson, MD**[‡], **James C. Carr, MD**[*], and **Debiao Li, PhD**[*,†]

[*]Department of Radiology, Northwestern University, Chicago, Illinois

[†]Department of Biomedical Engineering, Northwestern University, Chicago, Illinois

[‡]Department of Medicine, Northwestern University, Chicago, Illinois

Abstract

Purpose—X-ray angiography is currently the standard test for the assessment of coronary artery disease. A substantial minority of patients referred for coronary angiography have no significant coronary artery disease. The purpose of this work was the evaluation of the accuracy of a three-dimensional (3D) breathhold coronary magnetic resonance angiography (MRA) technique in detecting hemodynamically significant coronary artery stenoses in a patient population with x-ray angiographic correlation.

Materials and Methods—Sequential subjects (n = 33, M/F = 22/11, average age = 57) who were referred for conventional coronary angiography were enrolled in the study. The study protocol was approved by our institutional review board. Each subject gave written informed consent. Volume-targeted 3D breathhold coronary artery scans with ECG-triggered, segmented True Fast Imaging with Steady-state Precession (TrueFISP) were acquired for the left main (LM), left anterior descending (LAD), and right coronary arteries (RCAs). Coronary MRA was evaluated with conventional angiography as the gold standard.

Results—The overall sensitivity, specificity, accuracy, positive predictive value (PPV), and negative predictive value (NPV) for diagnosing any hemodynamically significant coronary artery disease (50% diameter reduction) with coronary MRA was 87%, 57%, 72%, 68%, and 80%, respectively. The sensitivity of the technique in the LM, LAD, and RCA was 100%, 83%, and 100%, respectively. The NPV of the technique in the LM, LAD, and RCA was 100%, 82%, and 100%, respectively.

Conclusions—Three-dimensional breathhold True Fast Imaging with Steady-state Precession is a promising technique for coronary artery imaging. It has a relatively high sensitivity and NPV.

Reprints: Debiao Li, PhD, Department of Radiology, Northwestern University, 448 East Ontario Street, Suite 700, Chicago, IL 60611. d-li2@northwestern.edu.

Results of this study warrant further technical improvements and clinical evaluation of the technique.

Coronary artery disease is the leading cause of death in both men and women in the United States.[1] Cardiac catheterization with conventional coronary angiography is currently the standard test for the assessment of coronary artery disease. Although various screening tests are available, a substantial minority of patients referred for coronary angiography have no significant coronary artery disease.[2] A noninvasive and accurate method of directly detecting functionally significant coronary artery disease would therefore be highly desirable.

Magnetic resonance imaging (MRI) has recently gained wide acceptance in cardiovascular disease examinations. Substantial progress has been made in developing MRI techniques for imaging coronary arteries in the past 10 years. These techniques can be divided into 2 major approaches based on the methods used for reducing respiration-related motion effects: free-breathing techniques with navigator echo-guided slice correction and breathhold techniques. Encouraging results have been shown using the free-breathing approach to detect significant coronary artery disease.[3–5] One of the shortcomings of the free-breathing approach is the relatively long imaging time per scan. Suboptimal image quality may result if heartbeat or breathing pattern changes substantially during data acquisition.

With the improved gradient system in recent MRI scanners, it is now possible to obtain three-dimensional (3D) images within a single breathhold.[6] However, with the conventional gradient-echo sequence Fast Low Angle Shot (FLASH), the signal-to-noise ratio (SNR) and spatial resolution are limited because of the constraint of the imaging time.[7] Administration of MR contrast media has substantially improved the SNR and contrast-to-noise ratio (CNR) of coronary arteries.[8–12] However, the number of contrast-enhanced breathhold scans in an imaging session was limited by the total contrast volume allowed per subject. Potential errors in time delay between contrast administration and start of data acquisition may also result in suboptimal image quality.

True Fast Imaging with Steady-state Precession (True-FISP) has been widely used in cardiac MR imaging in recent years.[13–15] A fat saturated, segmented 3D TrueFISP technique has been developed for breathhold volume-targeted coronary artery imaging.[16,17] It produces images with inherently higher coronary artery SNR and CNR than FLASH, and it does not require the administration of MR contrast media to obtain improved SNR and spatial resolution. The purpose of this work was to evaluate TrueFISP breathhold coronary MR imaging in a patient population with x-ray angiographic correlation.

MATERIALS AND METHODS

Thirty-three sequential subjects who were referred for conventional coronary angiography, and who had no history of previous coronary angioplasty or coronary stenting and no MR

contraindications were enrolled in the study, including 22 men and 11 women whose average age was 57 years (range, 38–73 years). Coronary magnetic resonance angiography (MRA) and conventional angiography were performed within 3 days to 3 months (mean 7.5 days) of each other. There were no clinical events and medication change between the 2 examinations. The study protocol was approved by our institutional review board. Each subject gave written informed consent.

The MRI examinations were performed on a 1.5 T whole body scanner (MAGNETOM Sonata, Siemens Medical Solutions, Erlangen, Germany) with a gradient subsystem of maximum gradient strength of 40 mT/m and maximum gradient slew rate of 200 mT/m/ms. A cardiac phased array coil with 12 elements (6 anterior, 6 posterior) was used for radiofrequency signal reception. An ECG-triggered, magnetization-prepared, segmented, 3D TrueFISP technique with fat saturation was used for imaging the coronary arteries.[16]

Two targeted scans were acquired in each patient, one to cover the left main (LM) and left anterior descending (LAD) coronary arteries and the other to cover the right coronary artery (RCA). For imaging plane localization, one or more overlapping low-resolution 3D TrueFISP scans were first acquired in a transverse plane at the level of the main coronary arteries. The parameters for the scans were as follows: repetition time (TR)/echo time (TE) = 2.7/1.0 milliseconds, flip angle = 70 degrees, field of view (FOV) = 255×300 mm^2, data acquisition matrix size = 90×256, number of lines acquired per heartbeat = 45, readout bandwidth = 980 Hz/pixel. Asymmetric sampling[17] was used to reduce TR, with 48 points collected before the echo and 128 points after the echo in a 256-point image reconstruction matrix. A total of 12 partitions (interpolated to 24) were acquired with a slab thickness of 60 mm. The breathhold time was 24 cardiac cycles during suspended inspiration. To determine the imaging plane orientation and position for a targeted coronary artery, 3 points in the proximal, mid, and distal segments of the coronary artery were selected manually in 3 different images of the localizer scan. The 3-point plane planning tool prescribes an imaging plane for the subsequent high-resolution scan. High-resolution coronary artery imaging had the following parameters: TR/TE = 3.5/1.4 milliseconds, flip angle = 70 degrees, FOV = $(180–250) \times (380–400)$ mm^2, acquisition matrix size = $(160–175) \times 512$, lines per cardiac cycle = 35–43 depending on heart rate, readout bandwidth = 650 Hz/pixel, slab thickness = 18 mm, number of partitions = 6 (12 interpolated), in-plane resolution = $(1.0–1.6) \times (0.74–0.78)$ mm^2, scan time = 24–30 heartbeats during suspended inspiration. The number of lines acquired per cardiac cycle was varied with the R-R interval of the patient to maximize imaging efficiency and to minimize cardiac motion effects. The total number of heartbeats required for each scan varied accordingly, within a patient's comfortable breathhold duration. All coronary MRA data were transferred to a Siemens workstation (Leonardo, Siemens Medical Solutions). Maximum intensity projections with a slice thickness of 3–5 mm were created on the workstations. Maximum intensity projections and original raw images were used for image analysis.

The conventional x-ray coronary angiograms were reviewed by 2 experienced cardiologists in consensus by using the quantitative coronary analysis method. The presence and site of any hemodynamically significant stenosis (50% diameter reduction) were recorded.

The coronary MRA images were reviewed by 2 experienced MRA reviewers by consensus, blinded to the results of the conventional angiography. Image quality was first graded on a scale of 1 to 5 (1 = very poor, 2 = poor, 3 = fair, 4 = good, 5 = excellent). Images with a grade 1 or 2 were excluded from further analysis. For images with a quality grade of 3 or above, the presence and site of any hemodynamically significant stenosis were recorded. Prevalence, sensitivity, specificity, accuracy, positive predictive value (PPV), and negative predictive value (NPV) of the MRA in detecting hemodynamically significant stenoses in the visualized segments of the coronary arteries were calculated using results from the conventional angiography as the reference.

RESULTS

Four of 33 subjects were eliminated from the study due to either unexpected claustrophobia or difficulty obtaining a consistent and reliable ECG signal. In the remaining 29 patients, 3 patients had only their LM and LAD vessels imaged by MRI because of time constraints. Three of 29 LMs, 1 of 29 LADs, and 7 of 26 RCAs had an MR image quality of 1 or 2 and were eliminated from further analysis. The mean study duration was 45 minutes (range, 20–61 minutes). The average number of breathholds for each patient was 9 (range, 5–14, including imaging plane localization and repeating scan for the same vessel due to suboptimal localization of coronary artery). The average breathhold duration was 22 seconds (range, 15–33 seconds).

The numbers and lengths of coronary arteries visualized with an image quality grade of 3 and above are shown in Table 1. The prevalence, sensitivity, specificity, accuracy, PPV, and NPV of MRA for detecting hemodynamically significant disease in the visualized segments of the coronary arteries are shown in Table 2.

Figures 1 and 2 show normal coronary magnetic resonance angiograms and the corresponding normal x-ray angiograms of the LM, LAD, and RCA in the same patient. Figures 3 and 4 show coronary magnetic resonance angiograms and the corresponding x-ray angiograms of the LM and LAD with various degrees of stenoses.

DISCUSSION

We have evaluated the 3D breathhold TrueFISP coronary MRA in a patient population with x-ray angiographic correlation. We found the technique to have high sensitivity and high NPV for hemodynamically significant coronary artery disease. Coronary MRA has been shown to be clinically useful in the assessment of anomalous coronary arteries.[18–20] However, with respect to the assessment of stenotic coronary artery disease, coronary MRA is currently regarded as an investigational technique. The relatively high overall sensitivity and NPV shown in this study are encouraging as a likely future role of coronary MRA would be to eliminate patients with no significant stenotic disease from further investigation.[2] Our results are similar to those reported in a multicenter study using the free-breathing, navigator echo-guided slice after approach.[4] Nevertheless, our study represents a single center clinical trial, which makes it easy to control the imaging protocol. Studies in other institutes are necessary to evaluate the reproducibility of the technique.

The LM, LAD, and RCA were routinely evaluated in our protocol. The left circumflex (LCx) artery was not evaluated, which represents a limitation of this study. There are no fundamental limitations to imaging the LCx using this technique. Based on our own experience, one of the major challenges in imaging the LCx is finding the appropriate orientation of the LCx, which applied to both breathhold and free-breathing approaches. The main purpose of the study was to assess the performance of the 3D breathhold TrueFISP technique in defining coronary artery stenoses, and we wanted to eliminate the complication of finding the proper LCx slab orientation in this feasibility evaluation of the technique. In addition, it has been shown that isolated LCx disease is relatively rare.[4,21] Patients with disease in the LCx are likely to have disease in other coronary arteries. In our study, 4 of 29 patients (14%) had hemodynamically significant disease in the LCx. Of these, all had significant disease elsewhere in their coronary circulation. Therefore, for the patient group in this study, visualization of the LM, LAD, and RCA has been sufficient for the potential decision of whether to direct the patients to conventional angiography. However, this needs to be assessed in a larger patient population in the future. Prior studies have had low accuracy for detecting coronary artery disease in the LCx,[4,10] and excluding the LCx in this study may potentially have biased the results of the study favorably. Further studies are required to assess the capabilities of this technique in defining functionally significant stenoses in all coronary arteries.

There was a relatively low overall prevalence of hemodynamically significant disease within the subject population, similar to the previous multicenter study.[4] However, this study population may not necessarily represent a limitation of the study because a likely future clinical role for coronary MRA is the elimination of patients who undergo conventional coronary angiography but do not have hemodynamically significant disease.[2] Therefore, our study population may represent the first group of patients to benefit from the clinical implementation of coronary MRA.

Overcoming the limitation of respiratory motion is the major challenge of coronary MRA. Although free-breathing technique allows higher spatial resolution than breathhold approach and a previous multicenter clinical trial using the navigator echo-guided motion-corrected free-breathing approach reliably identifies (or rules out) LM coronary artery or 3-vessel disease,[4,22] a potential limitation of the free-breathing approach is the relatively long imaging time, during which inconsistent heartbeat or breathing patterns may result in suboptimal image quality. Results of this study show that 3D breathhold imaging is a practical alternative approach to free-breathing imaging.

The major advantages of breathhold imaging are the short imaging time per 3D scan and the more complete elimination of the respiratory motion effects with cooperative patients. With the use of TrueFISP for data acquisition, SNR and CNR are generally adequate for submillimeter in-plane resolution. There is no requirement for contrast agents, so a 3D breathhold scan can be repeated if the image quality is suboptimal for any reason. However, the temporal resolution of the technique is limited. In this study, the acquisition period is 122–150 milliseconds (3.5×35–43), but for many normal people, the rest duration of coronary artery is about 90–120 milliseconds when the heart rate is 70 beats per minute, and the rest duration will decrease if the heart rate increases, so the image quality will be

impaired when heart rate increases. Because RCA has more extensive motion radius and shorter rest duration than other coronary arteries, we got a greater proportion of poor image quality in RCA in this study. In addition, the technique is susceptible to arrhythmias, incomplete breathhold, and magnetic field inhomogeneity, which resulted in poor image quality in 13% of the arteries imaged. A combination of the breathhold and free-breathing approaches may improve the success rate of coronary MRA.[23,24]

A shortcoming of the volume-targeted approach is the limited coverage of the coronary tree for each acquisition, thus accurate volume planning is required. The mean lengths of LAD and RCA in this study are shorter than that of the studies by Bogaert[25] (72 ± 15 and 90 ± 31 mm, respectively) and Kefer[26] (66 ± 12 and 115 ± 28 mm, respectively). The reason for this is that the respiration-gated technique was used in Bogaert and Kefer's studies.[25,26] Respiration-gated coronary MRA allows larger volume slab and higher resolution. A whole-heart coronary MRA approach has been developed in recent years which covers the entire coronary artery tree with a single acquisition.[27–29] However, the acquisition time of the whole-heart technique is still rather long, although the acquisition time has been substantially reduced with improved parallel acquisition techniques and radiofrequency coils.[30]

This technique is undergoing continuous technical improvements. Possible approaches to improving spatial resolution with 3D breathhold coronary artery imaging include parallel imaging,[31,32] partial Fourier reconstruction,[33,34] and undersampled projection reconstruction.[35,36] These methods can potentially achieve higher spatial resolution without increasing breathhold time. It is also possible to institute physiological approaches such as administering oxygen to increase breathhold duration and improve spatial resolution.[37] Newly developed blood pool contrast agents potentially allow improved SNR and CNR with repeated scans.[38–40] Finally, higher field strengths, such as 3.0 T imaging systems, offer the potential for further improvement in SNR, spatial resolution,[41] and imaging speed.[42,43] Further investigations are necessary to evaluate the possible benefits of these methods in a patient population.

An alternative approach to minimally invasive coronary artery imaging is multislice computed tomography, which has been practically used.[22] The state-of-the-art 64-slice computed tomography has shown very high diagnostic accuracy and image quality.[44] In addition, multislice computed tomography allows identification of atherosclerotic plaque components which is an important indication of plaque vulnerability.[45] A study comparing multislice computed tomography and MRI for coronary angiography showed that multislice computed tomography had higher sensitivity and similar specificity for detecting significant stenosis.[46] However, multislice computed tomography has the disadvantages of requiring the use of a potentially nephrotoxic contrast agent and ionizing radiation.

In this patient study, we achieved a relatively high sensitivity and NPV for hemodynamically significant stenosis using a 3D breathhold MRA approach. TrueFISP allows for 3D coronary artery imaging with submillimeter in-plane resolution within a single breathhold and does not require contrast agent administration. TrueFISP has inherently high SNR and therefore is particularly suitable for combination with techniques which improve

spatial resolution with a reduction in SNR. Results of this study warrant further technical improvements and clinical evaluation of the technique.

Acknowledgments

References

1. American Heart Association. Heart Disease and Stroke Statistics—2005 Update. Dallas, TX: American Heart Association; 2005.

2. Manning WJ, Edelman RR. Magnetic resonance coronary angiography. Magn Reson Q. 1993; 9:131–151. [PubMed: 8398716]

3. Ikonen AE, Manninen HI, Vainio P, et al. Three-dimensional respiratory-gated coronary MR angiography with reference to X-ray coronary angiography. Acta Radiol. 2003; 44:583–589. [PubMed: 14616201]

4. Kim WY, Danias PG, Stuber M, et al. Coronary magnetic resonance angiography for the detection of coronary stenoses. N Engl J Med. 2001; 345:1863–1869. [PubMed: 11756576]

5. Plein S, Jones TR, Ridgway JP, et al. Three-dimensional coronary MR angiography performed with subject-specific cardiac acquisition windows and motion-adapted respiratory gating. AJR Am J Roentgenol. 2003; 180:505–512. [PubMed: 12540462]

6. Wielopolski PA, van Geuns RJ, de Feyter PJ, et al. Breath-hold coronary MR angiography with volume-targeted imaging. Radiology. 1998; 209:209–219. [PubMed: 9769834]

7. van Geuns RJ, Wielopolski PA, de Bruin HG, et al. MR coronary angiography with breath-hold targeted volumes: preliminary clinical results. Radiology. 2000; 217:270–277. [PubMed: 11012456]

8. Goldfarb JW, Edelman RR. Coronary arteries: breath-hold, gadolinium-enhanced, three-dimensional MR angiography. Radiology. 1998; 206:830–834. [PubMed: 9494509]

9. Kessler W, Laub G, Achenbach S, et al. Coronary arteries: MR angiography with fast contrast-enhanced three-dimensional breath-hold imaging—initial experience. Radiology. 1999; 210:566–572. [PubMed: 10207446]

10. Regenfus M, Ropers D, Achenbach S, et al. Noninvasive detection of coronary artery stenosis using contrast-enhanced three-dimensional breath-hold magnetic resonance coronary angiography. J Am Coll Cardiol. 2000; 36:44–50. [PubMed: 10898411]

11. Li D, Carr JC, Shea SM, et al. Coronary arteries: magnetization-prepared contrast-enhanced three-dimensional volume-targeted breath-hold MR angiography. Radiology. 2001; 219:270–277. [PubMed: 11274569]

12. Yang CW, Carr JC, Francois CJ, et al. Coronary magnetic resonance angiography using magnetization-prepared contrast-enhanced breath-hold volume-targeted imaging. Invest Radiol. 2006; 41:639–644. [PubMed: 16829747]

13. Carr JC, Simonetti O, Bundy J, et al. Cine MR angiography of the heart with segmented true fast imaging with steady-state precession. Radiology. 2001; 219:828–834. [PubMed: 11376278]

14. Barkhausen J, Goyen M, Ruhm SG, et al. Assessment of ventricular function with single breath-hold real-time steady-state free precession cine MR imaging. AJR Am J Roentgenol. 2002; 178:731–735. [PubMed: 11856708]

15. Jung BA, Hennig J, Scheffler K. Single-breathhold 3D-trueFISP cine cardiac imaging. Magn Reson Med. 2002; 48:921–925. [PubMed: 12418009]

16. Deshpande VS, Shea SM, Laub G, et al. 3D magnetization-prepared true-FISP: a new technique for imaging coronary arteries. Magn Reson Med. 2001; 46:494–502. [PubMed: 11550241]

17. Deshpande VS, Shea SM, Chung YC, et al. Breath-hold three-dimensional true-FISP imaging of coronary arteries using asymmetric sampling. J Magn Reson Imaging. 2002; 15:473–478. [PubMed: 11948838]

18. McConnell MV, Ganz P, Selwyn AP, et al. Identification of anomalous coronary arteries and their anatomic course by magnetic resonance coronary angiography. Circulation. 1995; 92:3158–3162. [PubMed: 7586298]

19. Post JC, van Rossum AC, Bronzwaer JG, et al. Magnetic resonance angiography of anomalous coronary arteries. A new gold standard for delineating the proximal cours. Circulation. 1995; 92:3163–3171. [PubMed: 7586299]

20. Taylor AM, Thorne SA, Rubens MB, et al. Coronary artery imaging in grown up congenital heart disease: complementary role of magnetic resonance and x-ray coronary angiography. Circulation. 2000; 101:1670–1678. [PubMed: 10758049]

21. Hillis LD, Winniford MD. Frequency of severe (70% or more) narrowing of the right, left anterior descending, and left circumflex coronary arteries in right dominant circulations with coronary artery disease. Am J Cardiol. 1987; 59:358–359. [PubMed: 3812289]

22. Schuijf JD, Bax JJ, Shaw LJ, et al. Meta-analysis of comparative diagnostic performance of magnetic resonance imaging and multislice computed tomography for noninvasive coronary angiography. Am Heart J. 2006; 151:404–411. [PubMed: 16442907]

23. Foo TK, Saranathan M, Hardy CJ, et al. Coronary artery magnetic resonance imaging: a patient-tailored approach. Top Magn Reson Imaging. 2000; 11:406–416. [PubMed: 11153707]

24. Dewey M, Teige F, Schnapauff D, et al. Combination of free-breathhold and breathhlod steady-state free precession magnetic resonance angiography for detection of coronary artery stenoses. J Magn Reson Imaging. 2006; 23:674–681. [PubMed: 16568418]

25. Bogaert J, Kuzo R, Dymarkowski S, et al. Coronary artery imaging with real-time navigator three-dimensional turbo-field-echo MR coronary angiography: initial experience. Radiology. 2003; 226:707–716. [PubMed: 12601209]

26. Kefer J, Coche E, Legros G, et al. Head-to-head comparison of three-dimensional navigator-gated magnetic resonance imaging and 16-slice computed tomography to detect coronary artery stenosis in patients. J Am Coll Cardiol. 2005; 46:92–100. [PubMed: 15992641]

27. Weber OM, Martin AJ, Higgins CB. Whole-heart steady-state free processing coronary artery magnetic resonance angiography. Magn Reson Med. 2003; 50:1223–1228. [PubMed: 14648570]

28. Sakuma H, Ichikawa Y, Chino S, et al. Detection of coronary artery stenosis with whole-heart coronary magnetic resonance angiography. J Am Coll Cardiol. 2006; 48:1946–1950. [PubMed: 17112982]

29. Bi X, Deshpande V, Carr J, et al. Coronary MR angiography: a comparison between the whole-heart and volume-targeted methods using a T2-prepared SSFP sequence. J Cardiovasc Magn Reson. 2006; 8:703–707. [PubMed: 16891229]

30. Nehrke K, Börnert P, Mazurkewitz P, et al. Free-breathing whole-heart coronary MR angiography on a clinical scanner in four minutes. J Magn Reson Imaging. 2006; 23:752–756. [PubMed: 16557495]

31. Sodickson DK, Manning WJ. Simultaneous acquisition of spatial harmonics (SMASH): fast imaging with radiofrequency coil arrays. Magn Reson Med. 1997; 38:591–603. [PubMed: 9324327]

32. Pruessmann KP, Weiger M, Scheidegger MB, et al. SENSE: sensitivity encoding for fast MRI. Magn Reson Med. 1999; 42:952–962. [PubMed: 10542355]

33. Margosian P, Schmitt F, Purdy D. Faster MR imaging: imaging with half the data. Health Care Instrum. 1986; 1:195–197.

34. Xu Y, Haacke EM. Partial Fourier imaging in multi-dimensions: a means to save a full factor of two in time. J Magn Reson Imaging. 2001; 14:628–635. [PubMed: 11747016]

35. Peters DC, Korosec FR, Grist TM, et al. Undersampled projection reconstruction applied to MR angiography. Magn Reson Med. 2000; 43:91–101. [PubMed: 10642735]

36. Larson AC, Simonetti OP, Li D. Coronary MRA with 3D undersampled projection reconstruction TrueFISP. Magn Reson Med. 2002; 48:594–601. [PubMed: 12353275]

37. McCarthy RM, Shea SM, Deshpande VS, et al. Coronary MR angiography: trueFISP imaging improved by prolonging breath holds with preoxygenation in healthy volunteers. Radiology. 2003; 227:283–288. [PubMed: 12616011]

38. Li D, Zheng J, Weinmann HJ. Contrast-enhanced MR imaging of coronary arteries: comparison of intra- and extravascular contrast agents in swine. Radiology. 2001; 218:670–678. [PubMed: 11230638]

39. Huber ME, Paetsch I, Schnackenburg B, et al. Performance of a new gadolinium-based intravascular contrast agent in free-breathing inversion-recovery 3D coronary MRA. Magn Reson Med. 2003; 49:115–121. [PubMed: 12509826]

40. Deshpande VS, Cavagna F, Maggioni F, et al. Comparison of gradient-echo and steady-state free precession for coronary artery magnetic resonance angiography using a gadolinium-based intravascular contrast agent. Invest Radiol. 2006; 41:292–298. [PubMed: 16481912]

41. Stuber M, Botnar RM, Fischer SE, et al. Preliminary report on in vivo coronary MRA at 3 Tesla in humans. Magn Reson Med. 2002; 48:425–429. [PubMed: 12210906]

42. Santos JM, Cunningham CH, Lustig M, et al. Single breath-hold wholeheart MRA using variable-density spirals at 3T. Magn Reson Med. 2006; 55:371–379. [PubMed: 16408262]

43. Niendorf T, Hardy CJ, Giaquinto RO, et al. Toward single breath-hold whole-heart coverage coronary MR angiography using highly accelerated parallel imaging with a 32-channel MR system. Magn Reson Med. 2006; 56:167–176. [PubMed: 16755538]

44. Raff GL, Gallagher MJ, O'Neill WW, et al. Diagnostic accuracy of noninvasive coronary angiography using 64-slice spiral computed tomograpgy. J Am Coll Cardiol. 2005; 46:552–557. [PubMed: 16053973]

45. Leber AW, Becker A, Knez A, et al. Accuracy of 64-slice computed tomography to classify and quantify plaque volumes in the proximal coronary system: a comparative study using intravascular ultrasound. J Am Coll Cardiol. 2006; 47:672–677. [PubMed: 16458154]

46. Dewey M, Teige F, Schnapauff D, et al. Noninvasive detection of coronary artery stenoses with multislice computed tomography or magnetic resonance imaging. Ann Intern Med. 2006; 145:407–415. [PubMed: 16983128]
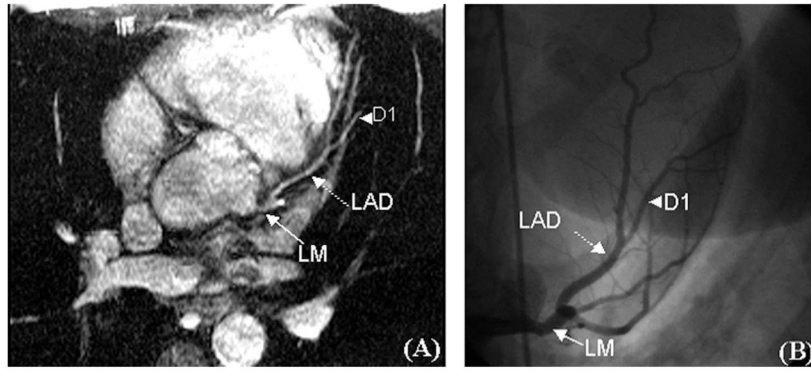
FIGURE 1.
Coronary angiograms of the LM and LAD in a 45-year-old with palpitations and a positive stress echocardiogram. A, The MRA image of the normal LM and LAD. B, The corresponding normal x-ray angiogram. D1 is the first diagonal branch of the LAD (arrowhead).
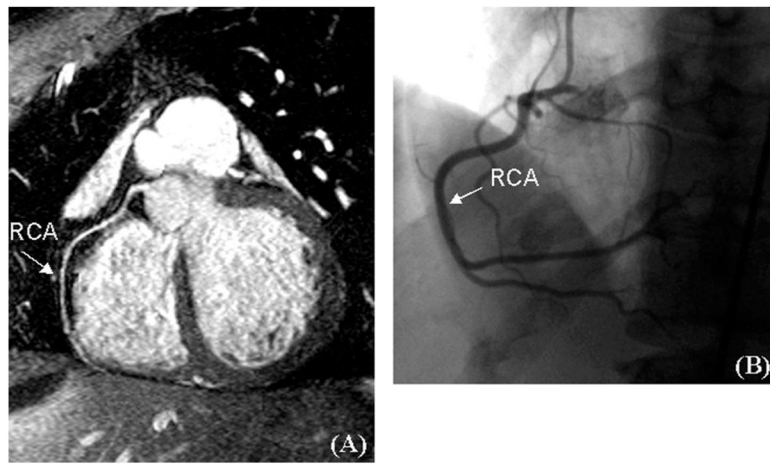
FIGURE 2.
Coronary angiograms of the RCA in the same subject as Figure 1. A, The MRA image of the normal RCA. B, The corresponding normal x-ray angiogram.
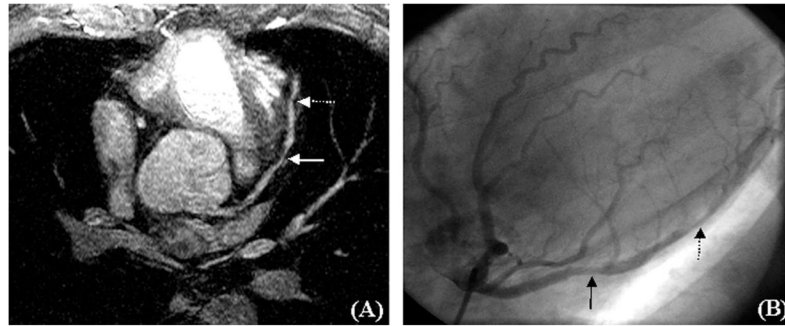
FIGURE 3.
Coronary angiograms of the LM and LAD in a 54-year-old asymptomatic male marathon runner who was referred for further evaluation of a high calcium score detected on screening computed tomography. A, The MRA image, and B, The x-ray angiogram. There is a 30% stenosis in the proximal LAD (solid arrows) and a 60% stenosis in the mid LAD (broken arrows).
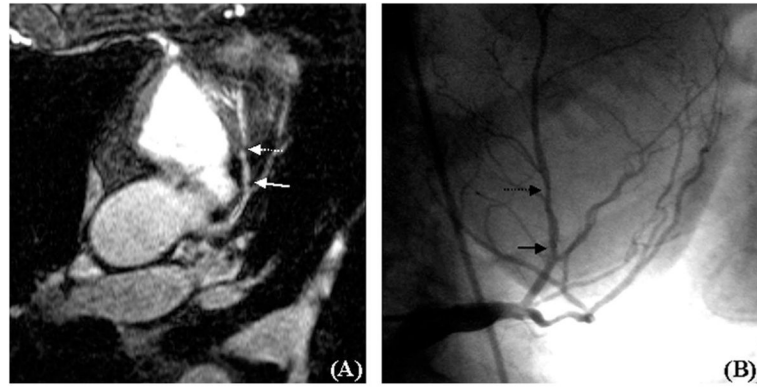
FIGURE 4.
Coronary angiograms of the LM and LAD in a 67-year-old man with unstable angina and a positive stress test. A, A coronary magnetic resonance angiogram. B, The x-ray angiogram. There is a 40% stenosis in the proximal LAD (solid arrows) and a 50% stenosis in the mid LAD (broken arrows).

TABLE 1

Numbers, Mean Lengths, and Range of Lengths of Coronary Vessels Visualized by Coronary Magnetic Resonance Angiography

Artery	Number	Mean Length Visualized (cm)	Range (cm)
RCA	19	6.4	2.9–10.3
LM	26	Full length	Full length
LAD	28	5.0	2.0–9.0

TABLE 2

Diagnostic Accuracy of Coronary Magnetic Resonance Angiography

Variable	Left Main Coronary Artery	Left Anterior Descending Coronary Artery	Right Coronary Artery	Any Coronary Artery Disease
No. true negatives	23	9	11	8
No. true positives	1	10	3	13
No. false negatives	0	2	0	2
No. false positives	2	7	5	6
Prevalence (%)	4	43	16	52
Sensitivity (%)	100	83	100	87
Specificity (%)	92	56	69	57
Accuracy (%)	92	68	74	72
Positive predictive value (%)	33	59	38	68
Negative predictive value (%)	100	82	100	80